© (2012) Trans Tech Publications, Switzerland
doi:10.4028/www.scientific.net/AMR.445.177

Constructing Surrogate Models for Springback in U-Bending Process

Deniz Bekar[1, a], Erdem Acar[1, b, *], Firat Ozer [1, c] and Mehmet Ali Guler[1, d]

[1]TOBB University of Economics and Technology, Department of Mechanical Engineering, Ankara, Turkey

[a]dbekar@etu.edu.tr, [b]acar@etu.edu.tr, [c]fozer@etu.edu.tr, [d]mguler@etu.edu.tr

*corresponding author, Sogutozu Cad. No: 43, Sogutozu, Ankara 06560 Turkey.

Phone: +90-312-292-4257, Fax: +90-312-292-4091

Keywords: U-bending, FEA, Springback, ANOVA, Surrogate models.

Abstract. In this study, surrogate models are constructed to approximate the behavior of simulation models for springback angles, sidewall curl, and sheet thickness reduction in U-bending process. The surrogate-modeling techniques used here are: (i) polynomial response surface (PRS), (ii) Kriging (KR) and (iii) radial basis functions (RBF). While constructing surrogate models, the following procedure is pursued. First, a set of training points is generated using Latin hypercube sampling method, and finite element simulations are performed at these points. Then, surrogate models are constructed utilizing the training data. The accuracies of the surrogate models are evaluated by using the leave-one-out cross validation errors. First-order PRS is found to be most accurate surrogate model for prediction of the springback angles, side wall curl, and sheet thickness reduction.

Introduction

In automotive and aerospace industry, the formed parts should meet the tolerance requirements in order to have a successful assembly. Inaccuracy of the geometries results in assembly problem and these problems can be reduced by compensating the springback, which is defined as the discrepancy between the desired and the formed shape. The springback is affected by mechanical and geometrical properties of the material, and the tooling parameters. The material parameters are the yield strength, anisotropy, and the hardening exponent [1]. The tooling parameters include stroke, blank holder force (BHF), and friction [2]. There are various methods to predict the springback behavior such as experimental, analytical and finite element analysis (FEA). Commercial FEA programs have been widely used in springback prediction studies. However, the accuracy of the computational model strongly depends on the number of integration points (NIP), the element formulation, the time step, and the contact algorithm [3, 4]. In this study, a coupled explicit–implicit solving algorithm [5] is used for springback calculations.

Solution of most engineering problems requires performing computationally expensive analyses (e.g., high fidelity finite element analysis for structural mechanics problems). Regular engineering practices such as evaluating the feasibility of many alternative design, exploration of design space, sensitivity analysis and design optimization become impractical as they involve performing huge number of simulations. When computational cost of the finite element simulations is expensive, the behavior of simulation models can be approximated by using surrogate models. Once constructed, surrogate models provide quick estimates to the solution of the problem. In this study, surrogate models are constructed to approximate the behavior of simulation models for springback angles, sidewall curl, and sheet thickness reduction in U-bending process. Three popular surrogate modeling techniques –polynomial response surface (PRS) [6], radial basis functions (RBF) [7], and Kriging (KR) [8] – are used to predict the above-mentioned outputs. A comprehensive review of several surrogate modeling, and design of experiments (DoE) techniques can be found in Ref. [9].

In this work, 12 parameters are considered as the essential process variables affecting the occurrence of springback angles, sidewall curl, and sheet thickness reduction. These mentioned parameters are; the blank holder force (*BHF*), the ratio of the final value of *BHF* (*BHF2*) to the initial value of *BHF* (*BHF1*) (*BHF2/BHF1*), the friction coefficient (f_s), the hardening coefficient (K), the hardening exponent (n), the ratio of clearance to the sheet thickness (c/t), the die radius (r_d), the punch radius (r_p), the sheet thickness (t), the anisotropy coefficients for three directions (0°, 45°, 90°) R_0, R_{45}, and R_{90}. To construct the surrogate models, first a set of training points is generated using Latin hypercube sampling method [10]. Then, the springback analysis is performed by using FEA to compute the responses at the training points. Finally, the surrogate models are generated. The most accurate surrogate model is determined by comparing mean absolute error (MAE) values of the fitted surrogate models. The performance (MAE) of each predictive model is estimated using leave-one-out cross-validation technique.

U-channel Forming. The geometrical parameters of the U-bending process are given in Fig. 1. The process is similar to the problem given in Numisheet 93. However, the blank material is a dual phase steel (DP 600). Parameters of the forming process and the dimensions of the blank are provided in Table 1.

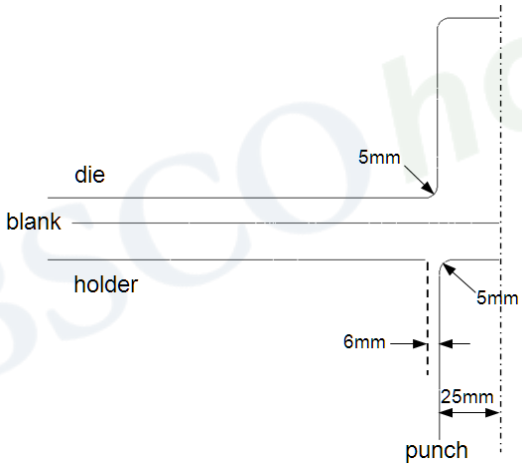

Figure 1. Tool geometries of the U-channel forming process

Table 1. Process parameters and dimensions of the blank

Stroke [mm]	Friction coefficient	BHF [kN]	Clearance (c) [mm]	Blank dimensions [mm]	Blank thickness [mm]	Tool velocity [mm/s]
70	0.12449	46.4 - 71*	1	35x350	0.8	20

*BHF is linearly increasing

FE analyses of the forming process and the springback have been performed by using the commercial FE code LS-DYNA. Since the blank is 0.8 mm in thickness, 7 integration points have been used in the FE analysis of the forming process. This NIP value is suitable when the computation time and accuracy are taken into account [11]. In the parametric analyses, several thickness values are used. When the thickness of the blank material is increased to 0.9 mm, more integration points should be used. This is due to the fact that unexpected deformations have been observed after springback simulation (Fig. 2.) when 7 integration points are used for 0.9 mm blank. Consequently, due to the variation of the blank thickness, NIP value is set to 11 in order to have consistent parametric analyses.

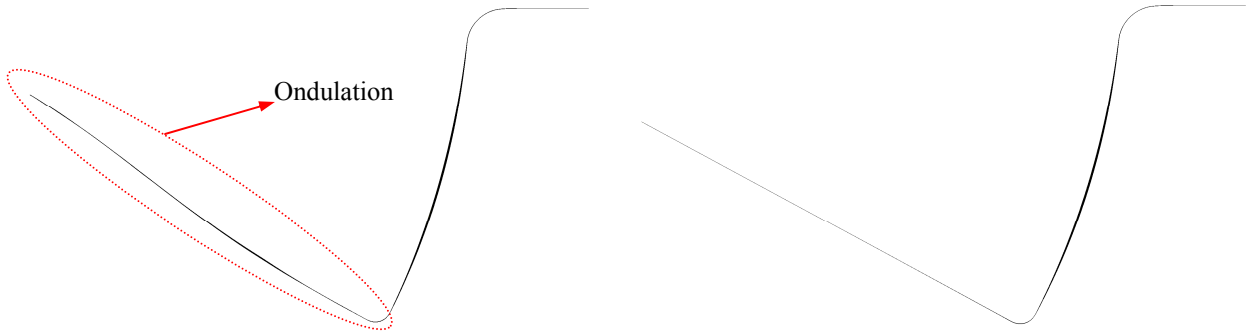

Figure 2. Comparison of NIP7 (left) and NIP11 (right) after springback simulation of a 0.9 mm thick DP600 blank

Validation of the FEA. Three-parameter Barlat yield criterion is decided as the material model in accordance with the anisotropic behavior of the blank (see Table 2). For the given process, 10 different parts were formed through rolling direction. Experiments were conducted at COSKUNOZ HOLDING A.S.

Table 2. Mechanical properties of the DP600 steel blank

σ_{YS} [MPa]	E [GPa]	ν	K [MPa]	n	ε_o	R_0	R_{45}	R_{90}
350	210	0.3	1076	0.189	0.002628	0.97	1.07	1.17

Springback angles and sidewall curl radii of both the experimental and LS-DYNA simulation results were measured according to the Numisheet93 procedure given in Fig. 3.

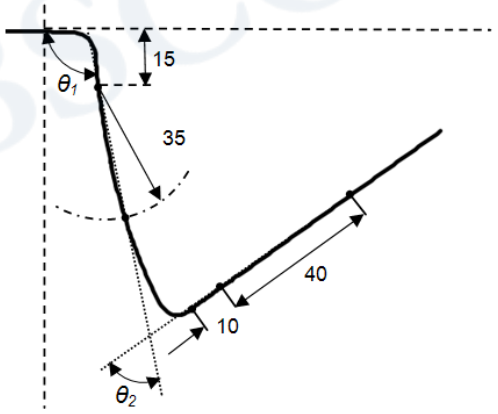

Figure 3. Procedure of the springback measurement

Several numbers of integration points, element size, and die velocity are examined in order to validate the FE analysis. When the accuracy and the computation time are considered, the best agreement between the FE results and the experiments have been obtained by using 1 mm quadrilateral elements, seven integration points and 1000 mm/s die velocity. Comparison of the FE analysis results with the experimental results is given in Table 3.

Table 3. Comparison of the FE analysis with the experiments

Measurement	Sidewall angle (θ_1)	Flange angle (θ_2)	Sidewall curl (ρ)
Experiment (average)	99.29	81.72	209.02
LSDYNA (FEA)	100.92	81.43	207.94

Surrogate Model Construction. Instead of performing computationally expensive FE simulations directly for engineering practices such as design space exploration, sensitivity analysis and design optimization, building a mathematical relation for the interested problems (sidewall angle (θ_1), flange angle (θ_2) side wall curl (ρ), sheet thickness reduction (TR)) both cuts down the computational cost and facilitates the understanding of the relationship between inputs (process variables) and outputs (responses). For that purpose, first a bunch of training points is generated by choosing an experimental design. After that, response values at these training points are computed using FE analyses, and a training set is formed. Finally, different surrogate models are fitted using the training set. The constructed models provide prediction of the response at any random point.

Design of Experiments (DoE). Latin hypercube sampling (LHS) method is used to generate 120 training points in this study. Sampling points are created using the distribution type of the process variables, which is assumed uniform between the minimum and maximum values shown in Table 4.

Table 4. Min. and max. values for process variables

Variable	Min.	Max.
BHF [kN]	40	50
BHF2/BHF1	1.3	1.5
f_s	0.10	0.15
K [MPa]	1000	1150
n	0.12	0.20
c/t	1	1.2
r_d [mm]	3	7
r_p [mm]	3	7
t [mm]	0.7	0.9
R_0	0.89	0.985
R_{45}	0.975	1.173
R_{90}	0.9764	1.1823

Surrogate Models. After choosing an experimental design type, θ_1, θ_2, ρ, and TR values at the training points are computed using LS-DYNA. Then, first-order PRS (PRS1), second-order PRS (PRS2), first-order stepwise regression (SWR1), second-order stepwise regression (SWR2), RBF, and KR surrogate model types with zeroth- and first-order trend models (KR0 and KR1) are constructed by using training points and the computed θ_1, θ_2, ρ, and TR values. The reader is referred to Appendix B of Ref. [12] for a brief description of the surrogate models used in this work.

Accuracy of the Surrogate Models. The accuracy of the constructed surrogate models are evaluated by using mean absolute leave-one-out cross-validation error metric, MAE. To calculate the MAE, first a surrogate model type is constructed N times (where N is the number of training points), while leaving out one of the training points as the validation data each time. Then error value is obtained using Eq. (1). In Eq. (1) y^i is the exact value of the response at the retained training point x_i and $\hat{y}^{(i)}$ is the predicted value of the response using surrogate model.

$$MAE = \frac{1}{N}\sum_{i=1}^{N}\left|\frac{y^i - \hat{y}^{(i)}}{y^i}\times 100\right| \quad (1)$$

Comparison of the MAE of the surrogate models are given in Table 5, which shows that the PRS1 model is the most accurate for the θ_1 prediction, *SWR is the most accurate model for both ρ and TR predictions*, and KR1 model is the most accurate model for the θ_2 prediction. However, when the computation costs of model construction are considered, Kriging models are very time-consuming while PRS models provide very quick model construction and response prediction. In addition, prediction errors are very close for PRS1 and KR1. Due to these two reasons, *PRS1 is selected as a prediction model for both θ_1, and θ_2.*

Table 5. Accuracies of different surrogate models constructed for θ_1, θ_2, ρ, and *TR*

	PRS1	PRS2	SWR1	SWR2	RBF	KR0	KR1
Accuracies of surrogate models for θ_1 prediction							
Mean absolute cross validation errors	**17,54**	34,58	17,68	56,27	22,41	28,06	17,55
Accuracies of surrogate models for θ_2 prediction							
Mean absolute cross validation errors	16,83	37,99	17,19	41,03	24,41	24,87	**16,78**
Accuracies of surrogate models for ρ prediction							
Mean absolute cross validation errors	19,67	59,67	**18,34**	58,21	25,74	23,86	19,71
Accuracies of surrogate models for TR prediction							
Mean absolute cross validation errors	8,73	14,50	**8,60**	18,95	16,59	25,41	8,68

Sensitivity Analysis. Since PRS1 model is decided to be used, the most influential variables can be found out by examining the coefficients in the polynomials (for nonlinear models, global sensitivity analysis would be required). Input values are normalized between 0 and 1 while constructing polynomials, so coefficients of the variables can be compared to each other to decide whether a parameter is essential or not. Table 6 provides the definitions for variables shown as *X1*, *X2*, etc.

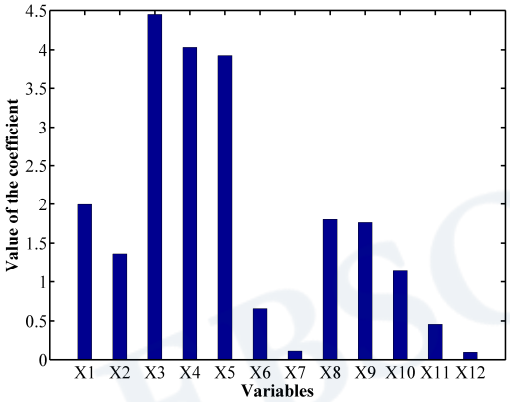

Figure 4. Effects of the variables for θ_1 prediction

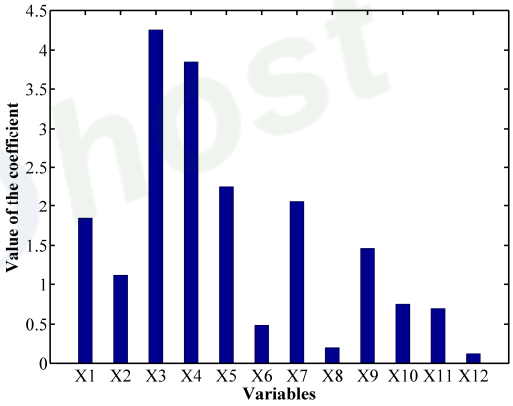

Figure 5. Effects of the variables for θ_2 prediction

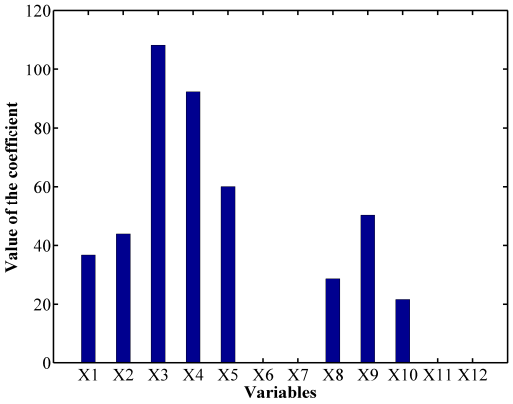

Figure 6. Effects of the variables for ρ prediction

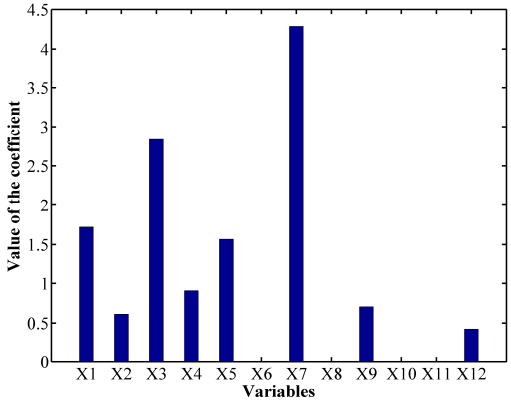

Figure 7. Effects of the variables for *TR* prediction

Table 6. Definitions for variables

Variable	*X1*	*X2*	*X3*	*X4*	*X5*	*X6*	*X7*	*X8*	*X9*	*X10*	*X11*	*X12*
Definition	*BHF*	*BHF2/BHF1*	f_s	*K*	*n*	*c/t*	r_d	r_p	*t*	R_0	R_{45}	R_{90}

As seen from Figure 4, f_s (*X3*), *K* (*X4*), *n* (*X5*) are essential for θ_1 prediction. Figure 5 shows that f_s (*X3*), *K* (*X4*), *n* (*X5*), and r_d (*X7*) are the most effective variables for θ_2 prediction. In addition, Figure 6 depicts that prediction of ρ depends on the same variables used for θ_1 prediction. For *TR* prediction, f_s (*X3*), and r_d (*X7*) are the most significant parameters (see Fig. 7).

Summary

In this work, three popular surrogate-modeling techniques (PRS, RBF, and KR) were used to determine the most accurate model for springback, sheet thickness reduction, and sidewall curl prediction in U-bending process. Mean absolute leave-one-out cross-validation error was computed to determine the accuracy of the surrogate models. First-order PRS model was found to be the most accurate model for the θ_1 and the θ_2 prediction, while first-order SWR was the most accurate model for the SWC and the TR.

Acknowledgements

The authors wish to thank the Scientific and Technological Research Council of Turkey (TÜBİTAK) for financial support under award MAG-109M078. We thank COŞKUNÖZ METAL FORM for conducting the experiments at their facilities. Authors would also like to thank Mustafa Yenice of COŞKUNÖZ METAL FORM for his help during the experiments.

References

[1] S.W. Lee, Y.T. Kim: Journal of Materials Processing Technology Vol. 187–188 (2007), pp. 89–93.

[2] T. de Souza, B. Rolfe: Journal of Materials Processing Technology Vol. 203 (2008), pp. 1–12

[3] L. Papeleux, J.-P. Ponthot: Journal of Materials Processing Technology Vol. 125–126 (2002), pp. 785–791.

[4] K.P. Li, W.P. Carden, R.H. Wagoner: International Journal of Mechanical Sciences Vol. 44 (2002), pp. 103–122.

[5] M.J. Finn, P.C. Galbraith, L. Wu, J.O. Hallquist, L. Lum, and T.-L. Lin: Journal of Materials Processing Technology, Vol. 50 (1995), pp. 395–409.

[6] R.H. Myers, D.C. Montgomery: *Response surface methodology: process and product optimization using designed experiments*. Wiley, NY (2002).

[7] M.D. Buhmann: *Radial basis functions: theory and implementations*. Cambridge University Press, NY (2003).

[8] T.W. Simpson, T.M. Mauery, J.J. Korte, F. Mistree: AIAA-98-4755.

[9] J.S Park: J. Stat. Plann. Infer. Vol. 39 (1994), pp. 95–111.

[10] M.D. McKay, R.J. Beckman, and W.J. Conover: Technometrics, 21(2) (1979), pp. 239-245.

[11] L. Chen, X. Qiu, S. Li, in: Proceedings of 7th International Conference and Workshop on Numerical Simulation of 3D Sheet Metal Forming Processes, Chapter 7 (2008).

[12] E.Acar, M.A. Guler, B. Gerçeker, M.E. Cerit, and B. Bayram: Thin-Walled Structures, 49(1), (2011), pp. 94-105.